

Supporting Information

Interplay between Intra- and Inter-Molecular Charge Transfer in the Optical Excitations of J-aggregates

Michele Guerrini,^{1,2,3} Caterina Cocchi,^{3*} Arrigo Calzolari,² Daniele Varsano,^{2*} and Stefano Corni^{2,4}

¹*Dipartimento FIM, Università di Modena e Reggio Emilia, Italy*

²*CNR Nano Istituto Nanoscienze, Centro S3, Modena, Italy*

³*Department of Physics and IRIS Adlershof, Humboldt-Universität zu Berlin, Berlin, Germany*

⁴*Dipartimento di Scienze Chimiche, Università di Padova, Italy*

Corresponding Authors: caterina.cocchi@physik.hu-berlin.de, daniele.varsano@nano.cnr.it

Section 1 – Additional information about the electronic and optical properties of the isolated push-pull monomer

Table S1 - HOMO-LUMO gap of the isolated push-pull monomer computed with different approximations for the exchange-correlation functionals as starting points for GW calculations (G_0W_0 and self-consistent on the eigenvalues only *ev-GW*). Calculations performed on relaxed geometry (cc-pVTZ basis set, force minimization threshold 10^{-4} Hartree /Bohr).

Starting point	DFT	G_0W_0	ev-GW
HARTREE-FOCK	8.42 eV	7.10 eV	6.91 eV
CAM-B3LYP	5.57 eV	6.46 eV	6.59 eV
B3LYP	3.25 eV	5.89 eV	6.44 eV
PBE0	3.56 eV	5.98 eV	6.47 eV
<u>PBE</u>	2.05 eV	5.19 eV	6.40 eV

Table S2 Comparison between the HOMO-LUMO gap of the monomer calculated from DFT with localized basis set using MOLGW and with plane-waves using the Quantum Espresso code. Calculations referred to the non-relaxed monomer geometry extracted from bulk J-aggregate.

<i>Code + convergence parameters</i>	<i>DFT gap</i>
<i>MOLGW (cc-pVTZ, PBE, all electrons, 10^{-8} Ry energy convergence accuracy)</i>	1.70 eV
<i>QUANTUM ESPRESSO (plane waves cut-off 60 Ry, PBE, optimized norm-conserving pseudopotentials, 10^{-8} Ry energy convergence accuracy). Supercell type: orthorhombic ($a=18 \text{ \AA}$, $b=18 \text{ \AA}$, $c=29 \text{ \AA}$) Vacuum layer of 20 \AA to avoid spurious interactions between the replicas.</i>	1.67 eV

Table S3 – Energy and composition of the first five excited state of the push-pull monomer $C_{24}H_{19}F_4N$, including the excitation energy and the weight given by the square of the normalized BSE coefficients. Only weights contributing more than 10% are reported. Calculations are performed on the non-relaxed geometry using the MOLGW code and the PBE functional as starting point for ev-GW calculations.

Excited state energy (eV)	Occupied level	Unoccupied level	Weight $A_{cv}^\lambda ^2$	Oscillator strength
$E^{M1} = 3.39$	HOMO	LUMO	0.83	3.50
$E^{M2} = 4.12$	HOMO	LUMO+3	0.73	0.08
$E^{M3} = 4.39$	HOMO-4	LUMO	0.16	0.09
	HOMO-1	LUMO	0.30	
	HOMO	LUMO+1	0.12	
	HOMO	LUMO+2	0.13	
$E^{M4} = 4.45$	HOMO-4	LUMO	0.21	0.30
	HOMO-1	LUMO	0.42	
	HOMO	LUMO+2	0.21	
$E^{M5} = 4.56$	HOMO-2	LUMO	0.63	0.04
	HOMO-2	LUMO+1	0.13	
$E^{M6} = 4.62$	HOMO-1	LUMO	0.11	0.04
	HOMO	LUMO+1	0.59	

Table S4 – Energy and composition of the first five excited state of the push-pull monomer $C_{24}H_{19}F_4N$, including the excitation energy and the weight given by the square of the normalized BSE coefficients. Only weights contributing more than 10% are reported. Calculations are performed on the relaxed geometry using the MOLGW code and the PBE functional as starting point for *ev*-GW calculations.

Excited state energy (eV)	Occupied level	Unoccupied level	Weight $ A_{cv}^\lambda ^2$	Oscillator strength
$E^M = 3.85$	HOMO	LUMO	0.76	3.36
$E^{M2} = 4.43$	HOMO	LUMO+3	0.64	0.02
$E^{M3} = 4.52$	HOMO-2 HOMO-2	LUMO LUMO+1	0.64 0.15	0.05
$E^{M4} = 4.63$	HOMO-5 HOMO-1 HOMO-1 HOMO	LUMO LUMO LUMO+2 LUMO+1	0.21 0.25 0.10 0.19	0.08
$E^{M5} = 4.68$	HOMO-5 HOMO-1	LUMO LUMO	0.20 0.46	0.20
$E^{M6} = 5.00$	HOMO HOMO	LUMO LUMO+1	0.10 0.49	0.08

Table S5 – Energy and composition of the first five excited state of the push-pull monomer $C_{24}H_{19}F_4N$, including the excitation energy and the weight given by the square of the normalized BSE coefficients. Only weights contributing more than 10% are reported. Calculations are performed on the relaxed geometry using the MOLGW code and the CAM-B3LYP functional as starting point for *ev*-GW calculations.

Excited state energy (eV)	Occupied level	Unoccupied level	Weight $ A_{cv}^\lambda ^2$	Oscillator strength
$E^M = 3.73$	HOMO	LUMO	0.768	2.44
$E^{M2} = 4.50$	HOMO HOMO	LUMO+2 LUMO+3	0.12 0.39	0.001
$E^{M3} = 4.58$	HOMO-5 HOMO-2 HOMO	LUMO LUMO LUMO+3	0.13 0.18 0.19	0.05
$E^{M4} = 4.60$	HOMO-2 HOMO-2	LUMO LUMO+1	0.39 0.12	0.01
$E^{M5} = 4.70$	HOMO-5 HOMO-1 HOMO	LUMO LUMO LUMO+1	0.11 0.44 0.15	0.05
$E^{M5} = 5.16$	HOMO-1 HOMO HOMO	LUMO LUMO LUMO+1	0.20 0.12 0.41	0.15

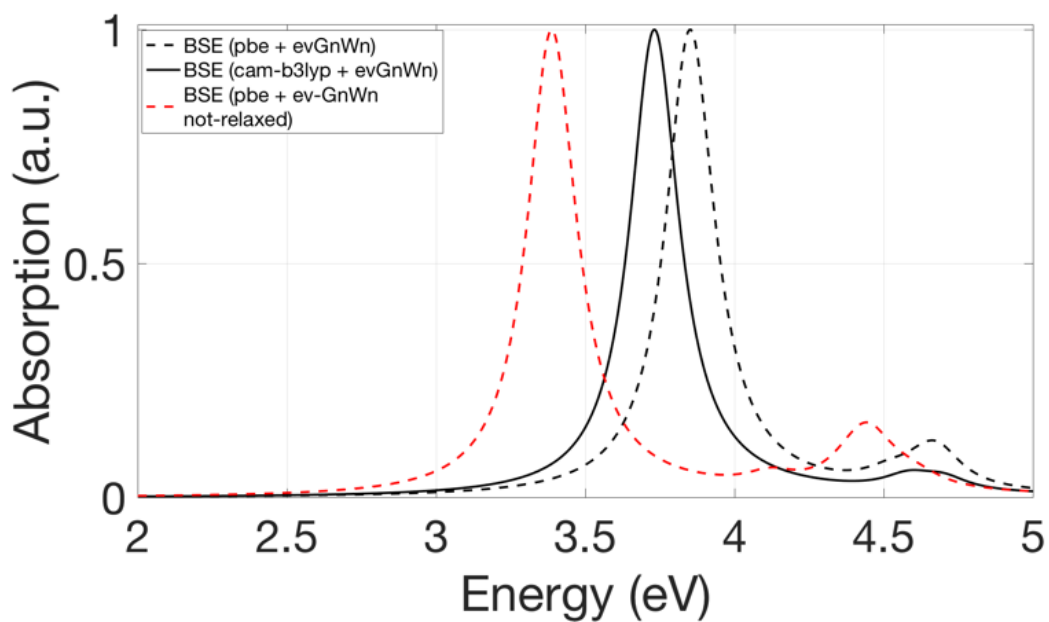


Figure S1 – BSE absorption spectra of the push-pull dye $C_{24}H_{19}F_4N$ obtained using two different xc-starting point functionals as starting point for ev-GW calculations: PBE (dashed line) and CAM-B3LYP (solid line). Calculations performed with the MOLGW cc-pVTZ basis in the Tamm-Dancoff approximation on the non-relaxed geometry in red and on the relaxed geometry in black.

Section 2 –Additional information about the electronic and optical properties of the J-aggregate

Table S6 - DFT and GW gaps for the J-aggregate. G_0W_0 is perturbative GW; $ev-G_nW_0$ is eigenvalues-only self-consistent GW where in each cycle one updates the energy eigenvalues only in the Green's function G while maintaining the screening W_0 as in the G_0W_0 first step; $ev-G_nW_n$ updates at each cycle the energy eigenvalues in both the Green's function G and the screening W

DFT (PBE)	G_0W_0	$ev-G_nW_0$	$ev-G_nW_n$
1.47 eV	3.21 eV	3.37 eV	3.37 eV

Table S7 - Energy and composition of the J and J_{CT} excitations of the J-aggregate, including the excitation energy, the \mathbf{k} -point at which the transition take place expressed in reciprocal crystal units (rcu), and the weight given by the square of the normalized BSE coefficients. Only weights larger than 2% are reported.

Excited state energy (eV)	Occupied band	Unoccupied band	\mathbf{k} -point (rcu)	$\epsilon_{ck}^{QP} - \epsilon_{vk}^{QP}$ (eV)	Weight $10 \times A_{cvk}^\lambda ^2$
$E^{J^1} = 2.786$	VBM	CBm	(-0.4, 0, 0)	3.21	0.75
	VBM	CBm	(0.4, 0, 0)	3.21	0.72
	VBM	CBm	(0.4, 0, -0.5)	3.22	0.66
	VBM	CBm	(-0.4, 0, 0.5)	3.22	0.64
	VBM-1	CBm+1	(-0.4, 0, 0.5)	3.23	0.64
	VBM-1	CBm+1	(0.4, 0, -0.5)	3.23	0.58
	VBM-1	CBm+1	(-0.4, 0, 0)	3.24	0.54
	VBM-1	CBm+1	(0.4, 0, 0)	3.24	0.53
$E^{J^3} = 2.813$	VBM-2	CBm+1	(-0.4, 0, 0)	3.33	0.24
	VBM-2	CBm+1	(-0.4, 0, 0.5)	3.34	0.24
	VBM-2	CBm+1	(0.4, 0, 0)	3.33	0.23
	VBM-3	CBm	(-0.4, 0, 0)	3.35	0.22
	VBM-3	CBm	(0.4, 0, -0.5)	3.34	0.22
	VBM-3	CBm	(-0.4, 0, 0.5)	3.34	0.22
	VBM-2	CBm+1	(0.4, 0, -0.5)	3.34	0.21
	VBM-3	CBm	(0.4, 0, 0)	3.35	0.21
$E^{J^5} = 2.903$	VBM	CBm	(-0.4, 0, 0)	3.21	0.66
	VBM	CBm	(-0.2, 0, 0)	3.27	0.53
	VBM	CBm	(-0.2, 0, 0.5)	3.28	0.49
	VBM	CBm	(-0.4, 0, 0.5)	3.22	0.45
	VBM	CBm	(0.4, 0.333, -0.5)	3.31	0.38
	VBM-1	CBm+1	(0.4, -0.333, -0.5)	3.32	0.38
	VBM-1	CBm+1	(-0.4, 0, 0.5)	3.23	0.37
	VBM	CBm	(0.4, 0.333, 0)	3.31	0.33
	VBM-1	CBm+1	(0.4, -0.333, 0)	3.32	0.32
	VBM-1	CBm+1	(-0.2, 0, 0.5)	3.30	0.26
	VBM-1	CBm+1	(-0.2, 0, 0)	3.32	0.24
	VBM-1	CBm+1	(-0.4, 0, 0)	3.24	0.21

	VBM	CBm	(0.4, -0.333, 0)	3.31	0.21
	VBM-1	CBm+1	(-0.4, 0.333, 0.5)	3.32	0.21
	VBM-1	CBm+1	(0.4, 0.333, 0)	3.32	0.21
	VBM	CBm	(-0.4, -0.33, 0.5)	3.31	0.21
$E^{J_{18}} = 3.03$	VBM	CBm+1	(0.4, 0, 0)	3.22	0.76
	VBM	CBm+1	(-0.4, 0, 0)	3.22	0.68
	VBM	CBm+1	(-0.2, 0, 0.5)	3.29	0.64
	VBM	CBm+1	(0.2, 0, -0.5)	3.29	0.63
	VBM-1	CBm	(0, 0, 0)	3.37	0.33
	VBM-1	CBm	(0.4, 0, -0.5)	3.23	0.22
	VBM-2	CBm	(-0.2, 0, 0)	3.34	0.21
	VBM	CBm+1	(0, 0, -0.5)	3.37	0.20

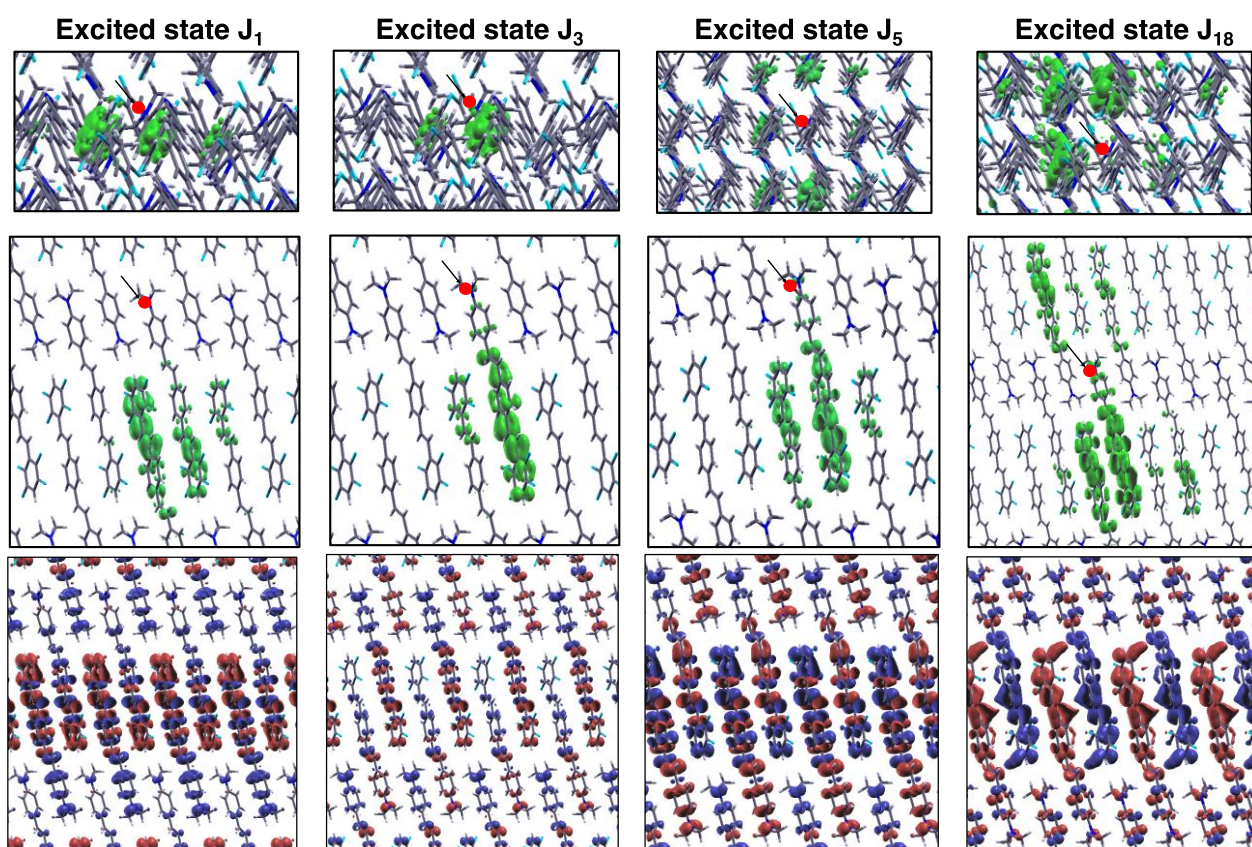


Figure S2 – Exciton probability densities with fixed hole position marked by the red dot (upper panels) and transition densities (lower panels) of the four excited states of J-aggregate, reported in Table S7. Isosurfaces fixed at 10% of the maximum value.